

# STM imaging of electronic waves on the surface of $\text{Bi}_2\text{Te}_3$

Zhanybek Alpichshev,<sup>1,2,3</sup> J. G. Analytis,<sup>1,2</sup> J.-H. Chu,<sup>1,2,4</sup> I.R. Fisher,<sup>1,2,4</sup>  
Y.L.Chen,<sup>1,2</sup> Z.X. Shen,<sup>1,2,3,4</sup> A. Fang,<sup>2,4</sup> and A. Kapitulnik<sup>1,2,3,4</sup>

<sup>1</sup>Stanford Institute for Materials and Energy Sciences,

SLAC National Accelerator Laboratory, 2575 Sand Hill Road, Menlo Park, California 94025

<sup>2</sup>Geballe Laboratory for Advanced Materials, Stanford University, Stanford, California, 94305

<sup>3</sup>Department of Physics, Stanford University, Stanford, CA 94305

<sup>4</sup>Department of Applied Physics, Stanford University, Stanford, CA 94305

(Dated: November 25, 2018)

$\text{Bi}_2\text{Te}_3$  has been proposed as a prototype topological insulator. Here we report scanning tunneling spectroscopy (STS) on high-quality doped- $\text{Bi}_2\text{Te}_3$  crystals. The perfect correspondence of the STS data to ARPES enables a unique identification of the different regimes measured in the local density of states (LDOS). LDOS oscillations near a step are observed and analyzed in the energy range that includes the bulk gap. We find that in the pure Dirac regime oscillations are strongly damped, supporting the hypothesis of a protected surface-state band. Pronounced oscillations at higher energies, close to the bulk conduction band, appear more regular while still exhibiting 2D character.

PACS numbers: 71.18.+y, 71.20.Nr, 79.60.-i

A new type of three-dimensional (3D) bulk insulating materials with surface Quantum Spin Hall Effect states protected by the time reversal symmetry has been recently predicted [3], and soon afterwards observed experimentally in BiSb bulk crystals [4]. Subsequently,  $\text{Bi}_2\text{Te}_3$  has been argued to be a three-dimensional topological insulator (TI), exhibiting a bulk gap and an odd number of relativistic Dirac fermion bands on the surface [1]. Indeed, recent angle resolved photoemission spectroscopy (ARPES), demonstrated that the surface state consists of a single nondegenerate Dirac cone [2]. Furthermore, with appropriate hole-doping, the Fermi level could be tuned to intersect only the surface states, indicating a full energy gap for the bulk states, thus suggesting that  $\text{Bi}_2\text{Te}_3$  is a three-dimensional TI. While ARPES could confirm the nature of the band, it is still a challenge to devise a proper measurement that will demonstrate unambiguously that  $\text{Bi}_2\text{Te}_3$  (or any other 3D TI system) possesses a surface state that is "protected."

In this paper we present scanning tunneling microscopy (STM) and spectroscopy (STS) on high-quality  $(\text{Bi}_{1-\delta}\text{Sn}_\delta)_2\text{Te}_3$ , and  $(\text{Bi}_{1-\delta}\text{Cd}_\delta)_2\text{Te}_3$  crystals (where  $\delta = 0.27\%$  for Sn doped and  $\delta = 1\%$  for Cd doped samples, both incorporated to compensate n-type doping from vacancy and anti-site defects.) First we show that the STM spectra exhibit perfect correspondence to ARPES data, hence enabling us to identify each region of the local density of states (LDOS) measured. Second, through the identification of cleavage steps, we analyze the occurrence of Friedel-oscillations associated with the surface state, concluding that within the main part of the Dirac band such oscillations are strongly damped, a hallmark of the lack of backscattering, hence supporting the hypothesis of a protected band. Finally, we show that in the region in which the Dirac band is strongly distorted as it meets the bulk-conduction band (BCB), normal Friedel-like os-

cillations associated with that surface state are recovered.

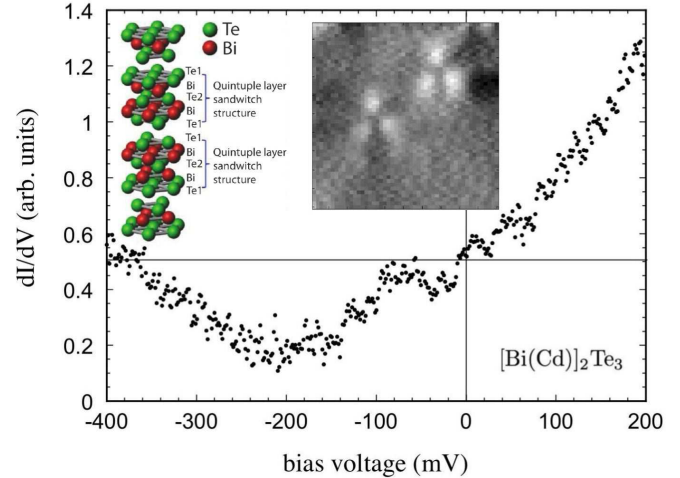


FIG. 1: A typical spectrum for Cd-doped  $\text{Bi}_2\text{Te}_3$ . Inset shows the crystal structure of  $\text{Bi}_2\text{Te}_3$ , and a  $72 \times 72 \text{ \AA}^2$  topograph of the surface, taken at a bias voltage  $V = +200 \text{ mV}$ , featuring two generic clover-shape impurities.

Samples for the present study are similar to those used in the ARPES study of Chen et al. [2]. A typical spectrum, taken at a random position on the surface of a cleaved crystal is shown in Fig. 1. The inset to that figure is a  $72 \times 72 \text{ \AA}^2$  topograph, taken with a bias-voltage of  $+200 \text{ mV}$  showing typical "clover-shaped" defects on the surface. The lack of atomic resolution at this bias voltage is due to the high density of free carriers. Topography on both, Sn-doped and Cd-doped  $\text{Bi}_2\text{Te}_3$  reported in this paper are similar to those previously obtained in STM studies of  $\text{Bi}_2\text{Te}_3$  and  $\text{Bi}_2\text{Se}_3$  [5, 6, 7].

At the outset, and to better understand the data that will be presented in this paper, it is instructive to understand the various regimes of the typical spectrum shown

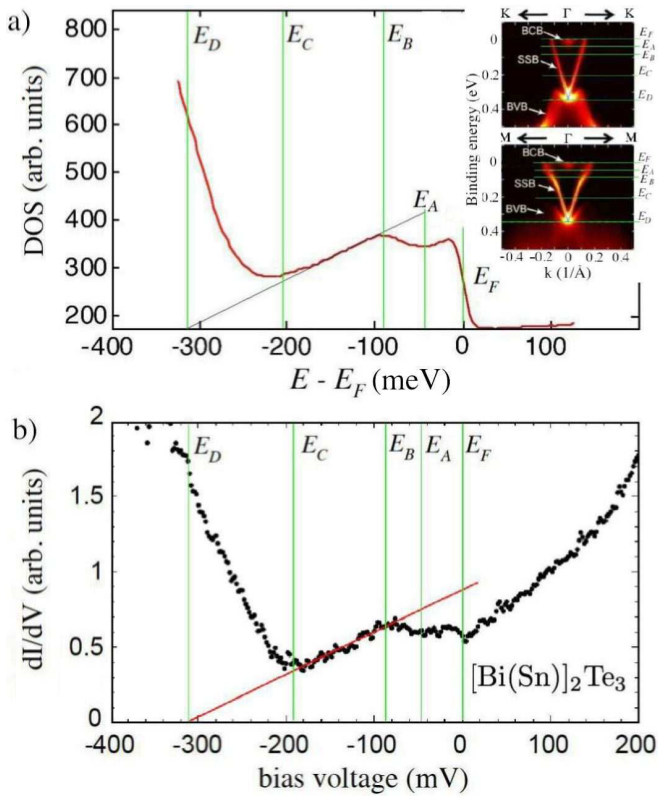


FIG. 2: DOS for Sn-doped  $\text{Bi}_2\text{Te}_3$ . a) Integrated DOS from ARPES. The various energies correspond to:  $E_F$  is the Fermi level;  $E_A$  is the bottom of the bulk conduction band;  $E_B$  is the point of the "opening up" of the surface state cone;  $E_C$  is the top of the bulk valence band; and  $E_D$  is the Dirac point. b) A local STM spectroscopy of a Sn-doped  $\text{Bi}_2\text{Te}_3$  showing the correspondence between the STM and ARPES data

in Fig. 1. This can be done by a direct comparison to ARPES data. Thus, integrating the ARPES  $E(\mathbf{k})$  data of Chen *et al.* [2] over the Brillouin zone, we obtain the density of occupied states at the surface of the sample. Fig. 2a is the result of this integration in the relevant energy range that includes the Dirac band which was found to reside in the  $\sim 250$  meV gap of this system. The directly measured LDOS of a similarly Sn-doped  $\text{Bi}_2\text{Te}_3$  crystal, as obtained by STM measurement is shown in Fig. 2b. Note that here we extend the data to positive bias, as STM can also obtain information about empty states. In both figures zero energy marks the Fermi level ( $E_F$ ). We also mark four other values of energies corresponding to the following important values.  $E_A$  corresponds to the bottom of the BCB as measured by ARPES and  $E_B$  corresponds to the point where the two-dimensional surface-state band (SSB) evolves from a linearly-dispersing band in the vicinity the bulk valence band (BVB), to a band with cross-sectional (constant-energy) hexagonal-star like shape (see ref. [2]). The linearly-dispersed Dirac band extends from its tip at  $E_D$  to  $E_B$ , while  $E_C$  denotes the top of the BVB. As can be

seen from the ARPES dispersion in Fig. 1a, the Dirac point is not exposed in this system, hence leaving us with only a relatively small range of pure linear LDOS expected from a Dirac dispersion (between  $E_C$  and  $E_B$ ).

To explore the properties of the quasiparticles that occupy the Dirac band, we searched for impurities and other defects in the crystals. In general interference patterns as a result of scattering from impurities and defects have shown to provide important information on the electronic structure of materials, especially surface states [8, 9, 10]. Unfortunately, attempts to observe quasiparticle-scattering interference effects from point impurities have so far failed, due to the very weak effect of non-magnetic impurities in this system. On the other hand, finite size defects such as steps and extended-range defects are visible in the sense that they produce marked effects on the LDOS in their vicinity.

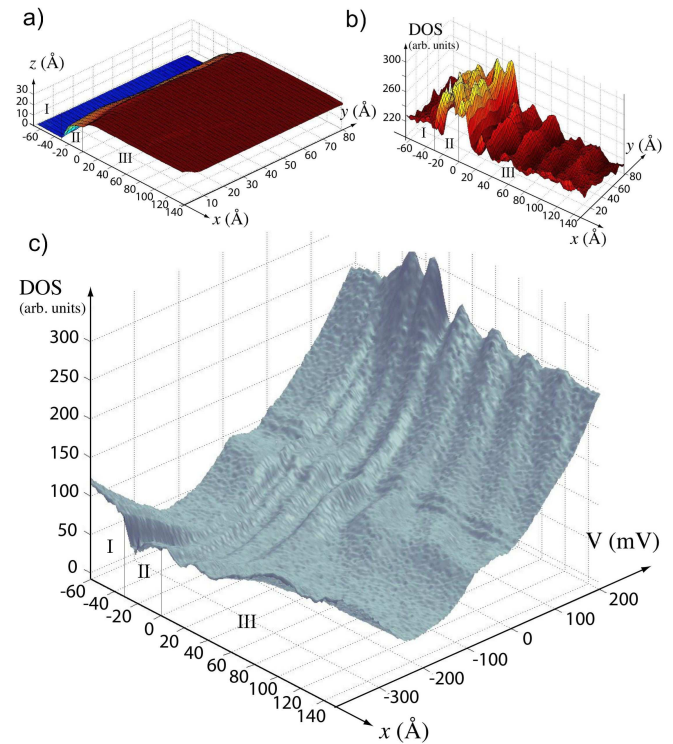


FIG. 3: a) Topography of the step. The total height of the step  $\sim 30$  Å corresponding to the thickness of the quintuple layer. The width of region II is  $\sim 20$  Å. b) Averaged spectroscopy as a function of distance from the step. The position of the step corresponds to "0" of the x-axis. Note the abrupt termination of the LDOS oscillations at  $E_B$ . (Visible features near  $E_F$  are due to convolution with the electronic spectrum of the tip arising from its sharp geometry).

Fig. 3a is a topography, showing a step defect that was obtained during the process of cleaving of the crystal. The down-step is marked as region-I in the figure. The total measured thickness of the step between regions I and III is  $\sim 30.5$  Å, in excellent agreement with the thickness of one unit cell [11] (i.e. three quintuples). Ex-

amination of the topography also reveals a partial cleavage area,  $\sim 6\text{\AA}$  thick, intermediate between regions I and III and we mark it as region-II. We will now concentrate on region-III in which this combined defect is expected to scatter quasiparticles and yield interference patterns that reflect the properties of the different voltage. We mark the beginning of the step with  $x = 0$  (though we note that since the edge of the step is not atomically smooth, this choice is arbitrary to within a few  $\text{\AA}$ ). We will explore the electronic structure along a straight section of the step, a strip which is  $80\text{\AA}$  wide and  $150\text{\AA}$  long.

The local variations of LDOS as a function of the lateral position across the step are demonstrated for the case of  $V = +200\text{ mV}$  in Fig. 3b. Averaging similar patterns over the width of the step for each energy in the interval between  $V = -400\text{ mV}$  and  $V = +200\text{ mV}$ , we obtain Fig. 3c. For all three figures we mark the three spatial regions as discussed above.

Careful examination of Fig. 3c yields the following observations: i) Friedel-like oscillations [12] that originate from the step are observed for all energies above  $E_B$ , which is the energy at which the SSB opens up; ii) the period of the oscillations in that region increases with increasing bias energy; and iii) the “normal” oscillation pattern terminates abruptly below  $E_B$  (i.e. for the linear dispersion region of the SSB), showing strongly attenuated oscillations with at most two visible peaks.

To further elucidate the development of oscillatory behavior of the electronic LDOS, we show in Fig. 4 a series of 10 energies spanning from the regime that includes the BVB to the one that includes the BCB. The first five panels (a-e) are in the regime of clear oscillations. Here we fit these curves to a simple Friedel-like formula with a  $1/x$  decay, appropriate for 1D oscillations. Such a fit agrees with a two-dimensional band, suggesting that all the observed oscillations originate from the SSB. In contrast, an attempt to fit the data with a  $1/x^2$  decay, appropriate for a three-dimensional band, fails as can be seen in Fig. 4a. While the oscillations seem to fit well the theoretical curve away from the step, the fit near the step is poor, especially close to  $x = 0$ . Indeed, we do not expect a good fit near the origin [8], due to the step’s height variation and its roughness (see Fig. 3a), both make it a “soft” boundary condition. Thus, to reduce the sensitivity to the details of the boundary, and since no theory exists to describe quantum oscillations due to a step in a TI, we use a rather arbitrary procedure in which for each energy that shows oscillations we locate the position of the second peak ( $x \equiv x_{2p}$ ) with respect to  $x = 0$ . Using the correspondence  $2k_F \times x_{2p} = 2 \times 2\pi$ , we also obtain a relation between  $k_F$  and energy which is plotted in Fig. 5 vs.  $E - E_F$ . The obtained  $E(k)$  dispersion shows remarkable correspondence to the dispersion of the SSB obtained by ARPES (Fig. 2). Moreover, while we have only a few points in the linear “Dirac-regime,” we also

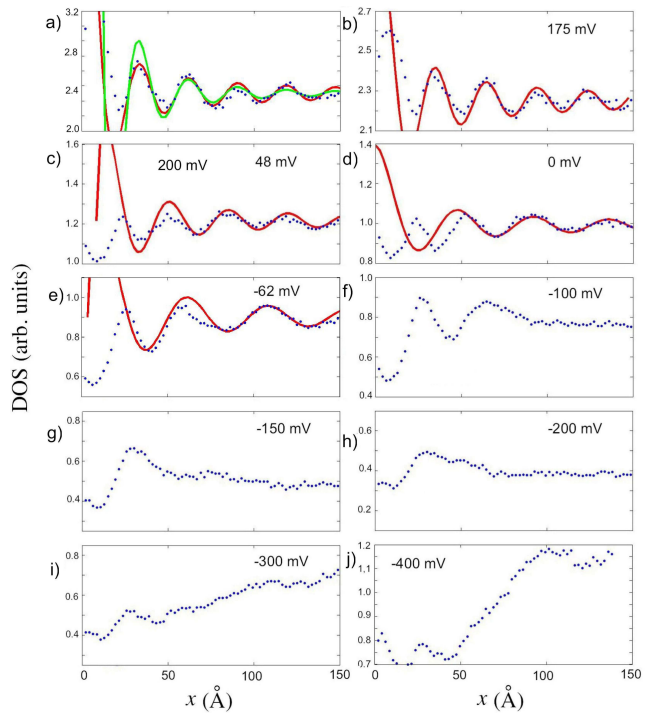


FIG. 4: Averaged LDOS as a function of distance from the step. a) fits to  $+200\text{ mV}$  showing decays of  $1/x$  - red line, vs.  $1/x^2$  green line. b), c), d), and e) correspond to energies above  $E_B$  showing well pronounced Friedel-like oscillations. Solid lines are the fits with  $\text{Sin}(x)/x$  type of curves, suggesting that scattered are the surface states. f), g), and h) correspond to energies within the Dirac cone, i) and j) correspond to energies overlapping with the bulk valence band.

note that a simple extrapolation to the origin ( $k = 0$ ) coincides with the observed Dirac point  $E_D$  and reproduce the slope of the Dirac cone as measured by ARPES [2]. All these are striking evidence that all the observed oscillations originate from the two-dimensional SSB.

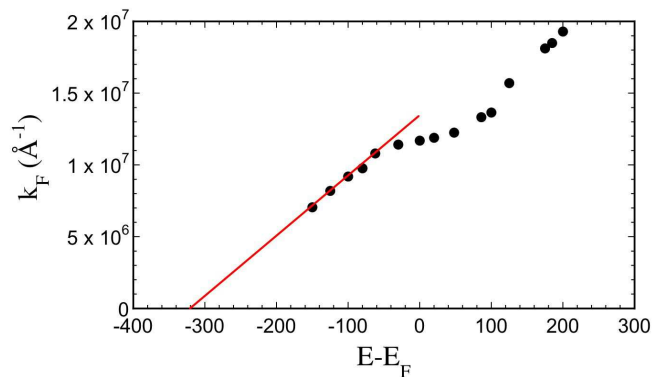


FIG. 5: Dispersion of the Fermi wavevector as determined by the position of the second peak from  $x = 0$ .

Since  $\text{Bi}_2\text{Te}_3$  is predicted to be a TI [1], possibly the most important observation to be made is that between

$E_C$  and  $E_B$  there are no slowly,  $1/x$ -like, decaying LDOS oscillations which would be expected for any “simple” surface state. This strongly supports the theoretical idea that pure surface states in TI systems should be protected from backscattering, and hence should not exhibit Friedel-oscillations, which are a consequence of the interference of incoming and backscattered waves. This “protection” results from the chiral character of the surface state, having a definite spin state. Thus, for scatterers that respect time reversal symmetry, any backscattering process should also include spin-flip in order to stay within the same chirality class. Since no such events are possible for non-magnetic defects, such as the step, no backscattering is allowed. However as is evident from Figs. 4f, g and h, the LDOS profile in the pure Dirac regime is not flat, suggesting possible fast-decaying oscillations below  $E_B$ . This unexpected effect may be explained by the observation that backscattering events are only forbidden classically, while quantum-mechanically second-order corrections allow for an oscillatory behavior that decays as  $1/x^2$  [13].

We turn now to address the nature of the oscillations above  $E_B$ . In principle, this energy is still within the SSB, and thus, at least below  $E_A$ , we do not expect any change in the oscillatory behavior as we cross this energy from below. However, two possible scenarios should be considered at this juncture. First, while the dispersion analysis presented above precludes pure bulk origin for the oscillations (as it would also require an unobserved  $k$ -divergence at  $E_A$ ), the BCB can still play a role in promoting oscillations if we assume that due to its presence, quasiparticles can be scattered from  $\mathbf{k}$  to  $-\mathbf{k}$  via intermediate states in BCB. Direct calculations of such an effect are rather cumbersome and thus beyond the scope of this present work. However, it is not impossible that such processes give rise to  $1/x$  type oscillations [13]. In such a scenario, the observed strong  $z$ -dispersion of the BCB [2] may account for the oscillations in the energy range between  $E_A$  and  $E_B$ , where there are supposedly no bulk states. Indeed,  $E_A$  was found to depend on photon energy, where more energetic and hence deeper probing photons revealed lower  $E_A$ , possibly coinciding with  $E_B$  in the limit of very large photon energy. Thus, despite the apparent distinction between  $E_A$  and  $E_B$  as seen in the inset of Fig. 2a, there is still some interaction between the exponentially decaying tail of the SSB and the BCB. This also implies that the transition between pure SSB and SSB+BCB regimes is a crossover whose width is determined by the penetration depth of the surface state.

Alternatively, we note that at  $E_B$ , the cross-section of the surface band changes character from a fully convex shape (smoothly evolving from a circle near the Dirac point to a hexagon higher up in the band) to a concave hexagram, acquiring rounded-tips along the  $\Gamma$ -M direction (Fig. 1f in ref. [2]). Thus, while below  $E_B$  the density

of states is uniform along the Fermi line, above  $E_B$  it is non-uniform, strongly suppressed in the tips of the hexagram along the  $\Gamma$ -M direction, leading to a negative deviation from linearity for the integrated LDOS (Fig. 1). The fact that the  $k_F$  values extracted from the fit for energies above  $E_B$  correspond to the dispersion of the SSB along  $\Gamma$ -M direction, i.e. the hexagram rounded tips, may provide an evidence that all observed oscillations originate from the SSB, and that the hexagram-tips of the Fermi-surface are responsible for the breakdown of chirality protection above  $E_B$ , possibly as a result of spin frustration at these low LDOS points.

In conclusion we have performed an STM measurements on Cd- and Sn-doped  $\text{Bi}_2\text{Te}_3$  samples. While within the main part of the Dirac band oscillations are strongly damped, supporting the hypothesis of a protected surface band, above a certain energy ( $E_B$ ) as this band opens up towards the bulk conduction band, oscillations of a more regular 2D character appear, suggesting that the chirality protection is lost above  $E_B$ .

Discussions with Qin Liu, Xiaoliang Qi and Shoucheng Zhang are greatly appreciated. This Work was supported by the Department of Energy Grant DE-AC02-76SF00515. ZA is supported by Stanford graduate Fellowship.

- 
- [1] Xiao-Liang Qi, Taylor L. Hughes and Shou-Cheng Zhang, Phys. Rev. B 78, 195424 (2008); Xiao-Liang Qi, T. L. Hughes, S. Raghu, and Shou-Cheng Zhang, Phys. Rev. Lett. 102, 187001 (2009).
  - [2] Y. L. Chen, J. G. Analytis, J. H. Chu, Z. K. Liu, S. K. Mo, X. L. Qi, H. J. Zhang, D. H. Lu, X. Dai, Z. Fang, S. C. Zhang, I. R. Fisher, Z. Hussain, Z. X. Shen, Science 325, 178-181 (2009).
  - [3] L. Fu and C.L. Kane, Phys. Rev. B 76, 045302 (2007).
  - [4] D. Hsieh, Y. Xia, L. Wray, D. Qian, A. Pal, J. H. Dil, J. Osterwalder, F. Meier, G. Bihlmayer, C. L. Kane, Y. S. Hor, R. J. Cava, and M. Z. Hasan, Science 323, 919 - 922 (2009).
  - [5] S. Urazhdin, D. Bilc, S. D. Mahanti, and S. H. Tessmer, Theodora Kyratsi and M. G. Kanatzidis, Phys. Rev. B 69, 085313 (2004).
  - [6] S. Urazhdin, D. Bilc, S. H. Tessmer, and S. D. Mahanti, Theodora Kyratsi and M. G. Kanatzidis, Phys. Rev. B 66, 161306(R) (2002).
  - [7] Y.S. Hor, A. Richardella, P. Roushan, Y. Xia, J.G. Checkelsky, A. Yazdani, M.Z. Hasan, N.P. Ong, R.J. Cava, arXiv:0903.4406 (2009).
  - [8] M. F. Crommie, C. P. Lutz, D. M. Eigler, Nature 363, 524 (1993).
  - [9] Y. Hasegawa and Ph. Avouris, Phys. Rev. Lett. 71, 1071 - 1074 (1993).
  - [10] P. T. Sprunger, L. Petersen, E. W. Plummer, E. Lægsgaard, F. Besenbacher, Science 275, 1764 (1997).
  - [11] L. E. Shelimova, O. G. Karpinskii, P. P. Konstantinov, E. S. Avilov, M. A. Kretova, and V. S. Zemskov, Inorganic Materials 40, 451 (2004), Translated from Neorganich-

- eskie Materialy 40, 530 (2004).
- [12] J. Freidel, Nuovo Cimento Suppl. 2, 287 (1958).
- [13] Qin Liu, Xiaoliang Qi and Shou-Cheng Zhang, private communication.